

Rapid thermal annealing effect on amorphous hydrocarbon film deposited by CH₄/Ar dielectric barrier discharge plasma on Si wafer: Surface morphology and chemical evaluation

Abhijit Majumdar,^{1,a)} S. R. Bhattacharayya,² and Rainer Hippler¹

¹*Institut für Physik, Ernst-Moritz-Arndt-Universität Greifswald, Felix-Hausdorff-Str. 6, 17489 Greifswald, Germany*

²*Surface Physics Division, Saha Institute of Nuclear Physics, 1/AF Bidhan Nagar, Kolkata 700 064, India*

(Received 29 July 2008; accepted 21 March 2009; published online 11 May 2009)

The effects of rapid thermal annealing (RTA) on amorphous hydrogenated carbon-coated film on Si wafer, deposited by CH₄/Ar dielectric barrier discharge plasma (at half of the atmospheric pressure), was examined. Bubbles-like structures were formed on the surface of the deposited carbon-coated film. The surface morphology studied by scanning electron microscopy (SEM), which showed that the effect of RTA on the film changing the morphological property drastically at 600 °C and most of the bubbles started evaporating above 200 °C. The inbuilt energy dispersive x-ray in SEM gives the quantitative analysis of the annealed surface. X-ray photoelectron spectroscopy results of the as-deposited films agree with the IR results in that the percent of Si-CH₃, Si-O-Si and C-O(H) stretching vibrational band in the film. Most of these bands disappeared as the sample was annealed at 600 °C in Ar medium. © 2009 American Institute of Physics. [DOI: 10.1063/1.3116734]

I. INTRODUCTION

There are great interests in hydrogenated silicon carbide composite materials (SiCO:H, SiC:H, SiC, C-SiOH, etc.) due to its potential application in electronics, optical devices, and antireflective coating for solar cells.¹ Moreover, silicon carbide composite materials are widely applicable as valid alternative to silicon (Si) for microelectromechanical systems (MEMS) operating in harsh environments due to its superior mechanical, physical, and chemical properties.²⁻⁴ SiOC:H composites operating at high temperatures requires knowledge of the mechanical as well as chemical properties of the material as a function of temperature. Although silicon based MEMS devices find such wide uses today, they lack high temperature capabilities with respect to morphological, chemical, mechanical, and electrical properties;⁵⁻⁷ Hydrogen attachment at the surface of the carbon film leads to the bubbles rings formation. In another way the bubble formation is commonly observed in oxide scales on polycrystalline SiC but is rarely found on single-crystal scales.⁸⁻¹⁰ It is possible to fabricate integrated circuits with these composite materials, which are operationally more robust than those in Si.¹¹ The industrial application is much more intense on the SiC due its wide band gap, high thermal conductivity, and high carrier ionization coefficient.¹² The SiC composite film is usually prepared by plasma enhanced chemical vapor deposition,¹³ hot wire chemical vapor deposition,¹⁴ radio frequency sputtering method,¹⁵ dielectric barrier discharge (DBD) plasma,^{16,17} etc.

The thin film deposition by DBD plasma has several interesting features. It offers attractive perspectives for the coating deposition and surface functionalization as it pro-

vides an easily applicable system in the industrial process.^{16,18-24} The most important feature is that the plasma reaction zone is confined on the surface of the electrode or substrate area.²⁵ It is very interesting to see that whether it is diffused carbon bubbles or combination of hydrocarbon bubbles (-CO:H) or carbonate bubbles (-CO₃ groups). Heat treatment is effective for the evaporation of the hydrogen/oxygen atoms from the surface of the deposited hydrocarbon film.

In the present work, amorphous hydrogenated carbon film on Si wafer has been deposited by DBD plasma and the film surface has been treated by rapid thermal annealing (RTA) effect to observe the change in the surface morphology and chemical bond properties. Surface morphologies were studied along with scanning electron microscopy (SEM) along with energy dispersive x-ray (EDX) analysis at room temperature as well as 200 and 600 °C, where as Fourier transform infrared (FTIR) absorption and x-ray photoelectron spectroscopy (XPS) analysis have been done at room temperature and at 600 °C for the chemical properties of the deposited composites.

II. EXPERIMENT

The hydrocarbon film was deposited on a 6 mm diameter *p*-type Si (100) substrate as well as the dielectric electrodes (upper electrode is Al₂O₃ and ground electrode is glass) by CH₄/Ar DBD plasma. The Si wafer used as a dummy substrate is located on the glass electrode. The experiment was performed at a pressure of 300 mbar and with a CH₄/Ar mixture ratio at 2:1. The characteristics of the hydrocarbon films deposited by varying CH₄/Ar gas mixture ratio, pressure, frequency, and time have been mentioned in our previous work.¹⁶ The experimental setup has been explained in detail elsewhere.²⁵ The average power executed on the sub-

^{a)} Author to whom correspondence should be addressed. Electronic mail: majumdar@physik.uni-greifswald.de. FAX: +493834864701.

strate during the deposition is about 4 W, where the peak to peak voltage was 10.5 kV at 4 kHz. The gap between two electrodes is variable according to the experimental requirement. The upper electrode is connected to a home-built high voltage power supply, while the lower electrode is grounded. The chamber is pumped by a membrane pump down to a base pressure of about 1 mbar. Pressure inside the plasma chamber was controlled by two gas flow controllers (for methane and argon) by an adjustable needle valve between the chamber and the membrane pump. The deposition time was typically about 6 h.

One of the deposited samples was heat treated by RTA (model: Jetfirst 100, Jipelec, Qualiflow, France) at temperatures of 200 °C and then at 600 °C for 3 min each in argon environment. The accuracy of temperature measurement was ± 2 °C. In every case of RTA the typical ramp-up and ramp-down temperature was ~ 25 °C/s.

The deposited as well as annealed (at 200 and 600 °C) films were examined by a scanning electron microscope with EDX analysis (model: Quanta 200 F). The SEM was operated at the energy of 10 keV and the typical magnifications were from 1500 \times to 8000 \times with a tilt angle of nearly 0°. EDX analysis was carried out mainly in spot mode with the typical time duration of 100 s. Apart from EDX, elemental analysis was also done after selecting a region from the mapping.

XPS measurements of the deposited film was performed on a VG Microtech (CLAM2: multitechnique 100 mm hemispherical electron analyzer) x-ray photoelectron spectroscope, using Mg K α radiation (photon energy 1253 eV) as the excitation source and the binding energy (BE) of Au (Au 4f $_{7/2}$:84.00 eV) as the reference. The XPS spectra were collected in a constant analyzer energy mode at a chamber pressure of 10 $^{-8}$ mbar and pass energy of 23.5 eV at 0.125 eV/step.

FTIR measurement was carried out by Perkin Elmer, Spectrum one in transmission mode at room temperature in the spectral range between 4000 and 400 cm $^{-1}$. All the FTIR spectra were recorded with a resolution of 2 cm $^{-1}$ using a Si wafer as a reference. The number of scans for each spectrum was automatically chosen and averaged in order to ensure an optimal signal-to-noise ratio. A linear baseline has been systematically subtracted from all the FTIR spectra in order to make the comparison among them more significant.

III. RESULTS AND DISCUSSION

A. Scanning electron microscopy and energy dispersive x-ray

From SEM analysis, the bubbles structure on the surface of the deposited amorphous silicon-carbon film has been observed.¹⁰ Figure 1(a) shows the SEM image of as-deposited film on the Si substrate in DBD plasma for about 6 h. Figures 1(b) and 1(c) show the SEM images of annealed film at 200 and 600 °C, respectively. The typical SEM image shown in Fig. 2(a) was taken from the central region of the deposited film. The morphology developed in the sample is nearly the same all over the sample. The sample is populated with circular carbon rich features of differential sizes.

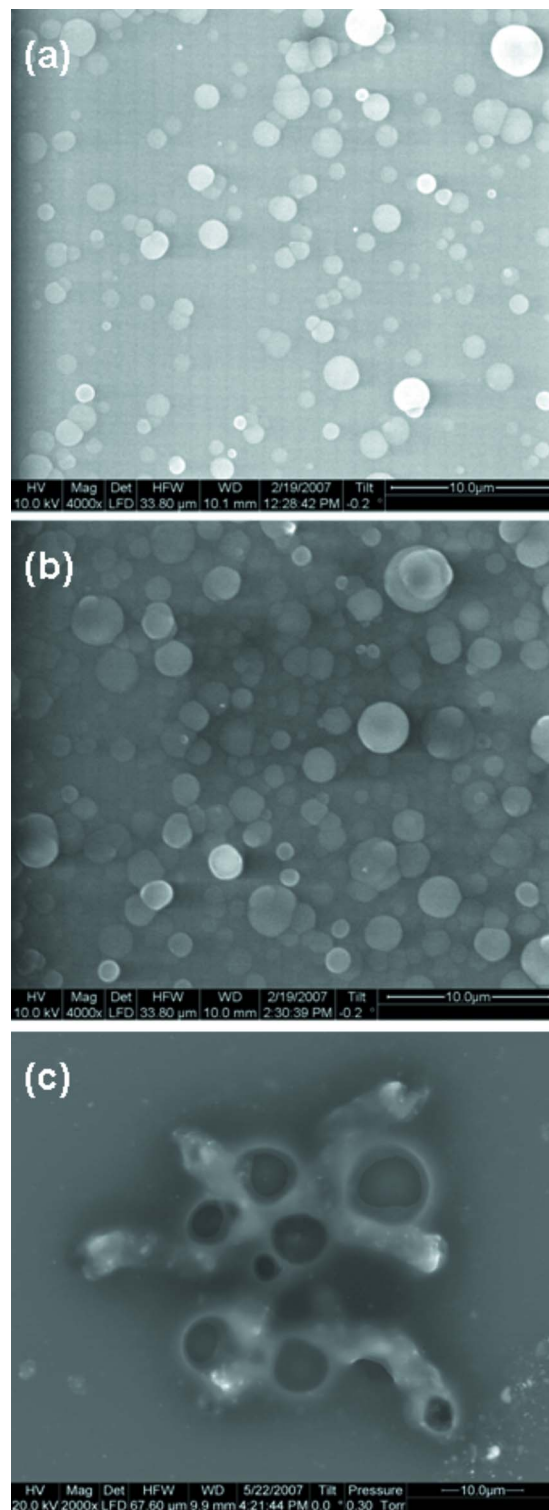


FIG. 1. (Color online) SEM images of SiCO:H film where (a) is the as deposited film, (b) is the annealed at 200 °C, and (c) is the annealed at 600 °C.

The sizes (diameters) of these circular spots vary from 250 nm to 3 μ m. Figure 3 shows the morphology of the annealed sample. The morphology shows that the changes are not appreciable as compared to the as-deposited one. Similar to the as-deposited sample, the circular spots (bubbles) also appeared in this annealed sample [Figs. 1(b), 2(a), and 3(a)]. The histogram of these spots is shown in Fig. 4, where the

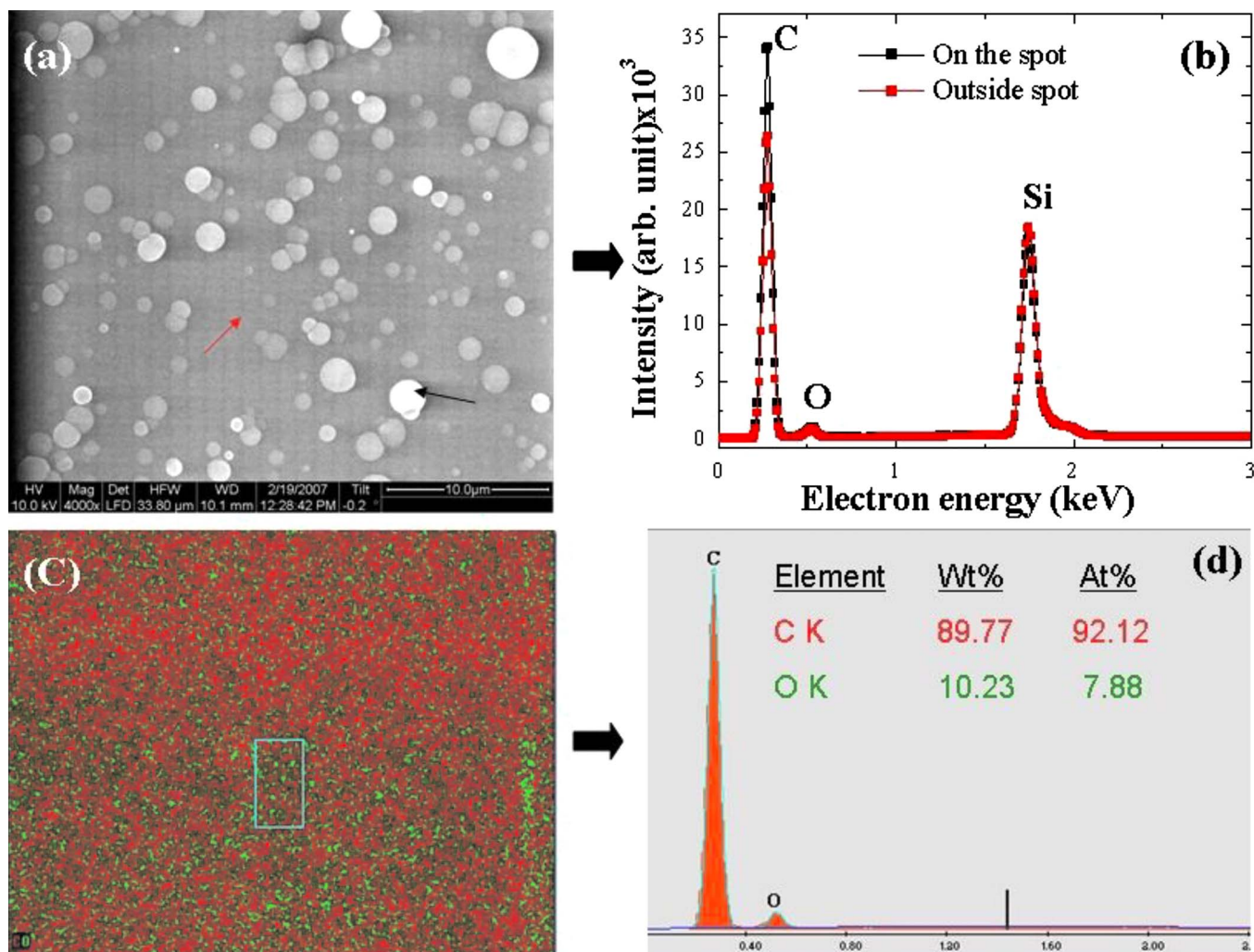


FIG. 2. (Color online) (a) SEM image of the as deposited sample (on the spot and outside the spot are denoted by arrows). (b) Corresponding EDX spectra. (c) Mapping image (selected rectangular area is analyzed). (d) Elemental analysis of the as-deposited SiCO:H film.

bubbles size of annealed film is partially shifted toward the larger size comparatively to the bubbles size of as-deposited film. In order to know the composition of the circular feature, along with the SEM, the EDX spectra were taken. Figures 2(b), 3(b), and 4 represent the EDX spectra from the sample as-deposited, 200 and 600 °C annealed samples, respectively. The lines are O K_{α} , C K_{α} , and Si K_{α} obtained from the EDX spectra taken in spot mode from the circular spots. From the EDX spectra, we can get the quantitative information about the stoichiometry of the sample on the spots. Figures 2(b) and 3(b) depict the EDX spectra taken from a circular feature in the spot mode. EDX spectra show that these spots are stoichiometrically carbon rich as compared to the EDX spectra from a region outside circular spots. The as-deposited SiC film was treated with RTA (for 3 min in Ar atmosphere) at 200 °C. However, the number density is increased here and many smaller spots are obtained. Annealing at a relatively higher temperature of 600 °C shows the morphology presented in Fig. 1(c). Remarkably this image shows almost a smooth surface, except a few ringlike features. It seems at this temperature, the circular spots are removed due to decomposition and evaporation of hydrocarbon from the sample surface. Table I gives the quan-

titative information of O, C, and Si for the sample of as deposited at 200 and 600 °C annealing. The information, as shown in Table I, clearly shows that the as-deposited and 200 °C annealed are carbon rich regions. Due to annealing, these carbon rich regions are depleted and the Si peak is increased. To simplify the EDX results quantification has been done and is shown in Table I.

The quantification of the elements in the films are as follows:

- As deposited: From the EDX spectra (Figs. 2 and 3) we got the information about the elemental quantification and we got the following atomic percentage. C (K_{α})-90.56 at. %, O (K_{α})-2.21 at. %, and Si (K_{α})-7.22 at. %; this elemental quantification shows that the film is populated by diffused carbon out of the hydrocarbon constituents.
- Annealed at 200 °C: C 92.39 at. %, O 2.87 at. %, and Si 4.74 at. % (from Table I). The EDX spectra (Figs. 3 and 5) show that in the as-deposited sample the carbon peak is dominated over silicon in accordance with the thick hydrocarbon layer formed on the Si substrate. As the annealing temperature is increased up to

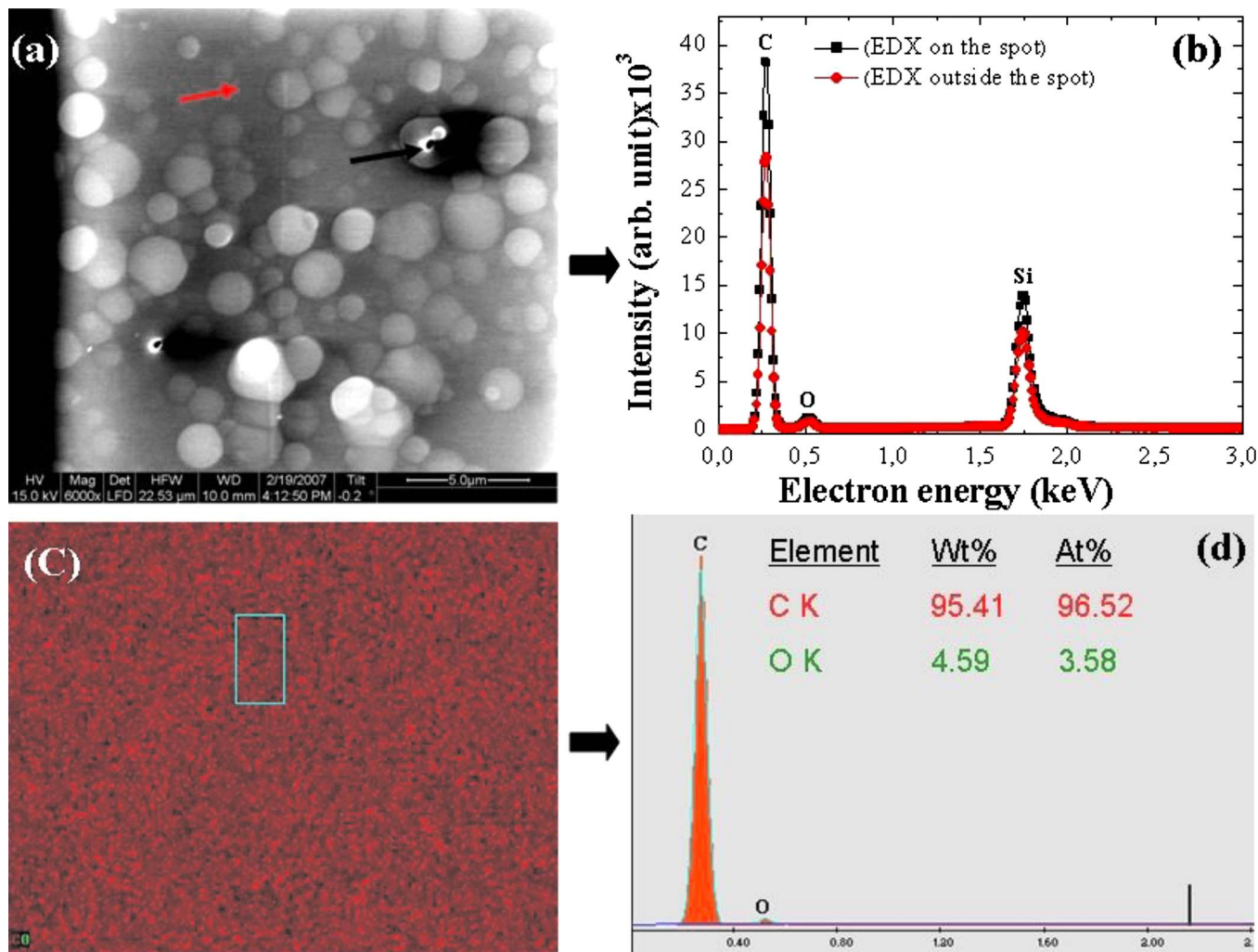


FIG. 3. (Color online) (a) SEM image of the SiCO:H film annealed at 200 °C. (b) Corresponding EDX spectra (on the spot and outside the spot are denoted by arrows). (c) Mapping image and (d) elemental analysis of the annealed SiCO:H film.

200 °C, carbon is diffused to form an agglomerated island of hydrocarbon due to surface activation energy. The EDX spectra on the selected carbon populated spot gives higher carbon intensity as compared to the as-deposited sample. As the annealing temperature is raised to 600 °C, most of the hydrocarbon bubbles are removed and the EDX spectra at this stage show a silicon dominated surface (Fig. 5).

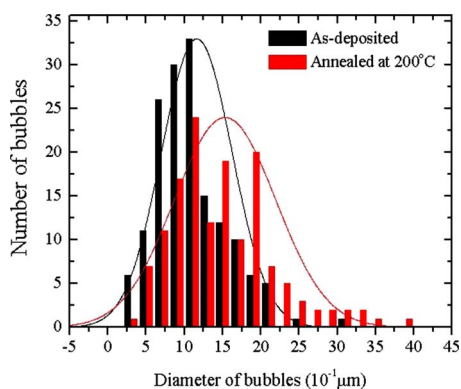


FIG. 4. (Color online) Histogram of the diameters of bubbles in SiCO:H film of as-deposited (black) and of annealed at 200 °C (red).

B. X-ray photoelectron spectroscopy

Chemical bonds among carbon, silicon, and oxygen can be deduced from a deconvolution of individual Si 2*p*, C 1*s*, and O 1*s* lines into Gaussian line shapes.^{16,17,26–28} In order to minimize the interference between the peaks during deconvolution, all spectra have been fitted with equal line widths (full width at half maximum, FWHM) of the concerned individual peak, thereby reducing the number of free parameters and yielding a more stable result. All fittings were obtained by constraining the FWHM to be equal to 1.90 eV. We considered that the surface spectrum was influenced by adsorbed molecules (e.g., oxygen, hydrogen). A noticeable

TABLE I. The quantitative information of O, C, and Si for the sample of as-deposited, annealed at 200 °C and 600 °C, and obtained from EDX spectra.

Sample	C K _α (at. %)	O K _α (at. %)	Si K _α (at. %)
As deposited	90.56	2.21	7.22
Annealed 200 °C	92.39	2.87	4.74
Annealed 600 °C	36.38	1.73	61.87

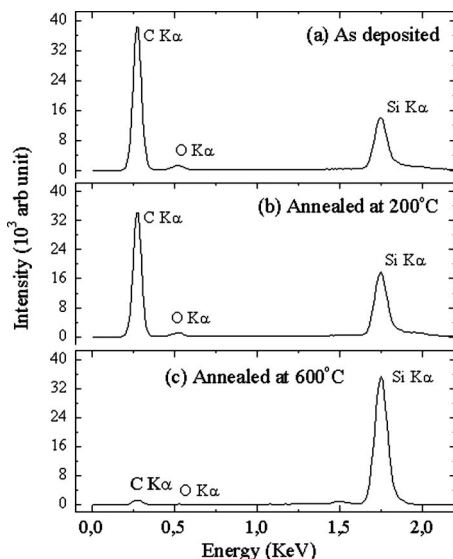


FIG. 5. EDX spectra of the SiCO:H film (a) from the as-deposited sample, (b) sample annealed at 200 and (c) at 600 °C.

chemical shift has been observed in the investigation of Si 2*p*, C 1*s*, and O 1*s* spectra due to an anomalous behavior of the surface charge distribution of the silicon substrate covered by carbon film. Si 2*p* with BE=99.50 eV was taken as reference. A chemical shift of 5.0 ± 0.5 eV was noted. The results presented below have been corrected for all the spectra by subtracting the experimentally observed shift.^{16,17}

From Fig. 6(a), we can see that the typical Si 2*p* spectra of the as-deposited film exhibit three subpeaks at 99.49, 100.24, and 103.49 eV, which are assigned to SiC, C–Si–O, and Si–O_x bonds, respectively.¹⁶ Similarly in the case of the annealed sample (at 600 °C), the peak intensity becomes higher than the previous and most of the peaks become flattened due to the partial chemical shift. The annealed sample exhibits three subpeaks at 97.7, 102.00, and 104.26 eV, which are assigned to SiC, C–Si–O, and Si–O_x bonds, respectively, obtained from Fig. 6(b).^{16,17} Due to annealing at 600 °C, the chemical properties of the film surface change, which could enhance the chemical shift (corresponding to the Si 2*p* BE). Moreover, the presence of hydrogen in the deposited film causes the drastic chemical shift; since the molecular bonds are generally and not purely covalent but also partially ionic. In our recent study it has been obtained by solid state nuclear magnetic resonance (NMR) analysis that there are large numbers of protons (H or H⁺) present in the deposited amorphous carbon nitride film.²⁹ Typical C 1*s* spectra are displayed in Figs. 7(a) and 7(b), in the case of as-deposited and annealed films, respectively. In the case of the as-deposited film, the C 1*s* spectrum exhibits four peaks at 284.00, 284.85, and 286.50 eV, which have been attributed to Si–C or Si–(CH₃)_x, C–C, and C–O(H) bonds, respectively.^{16,26,27,30} On the other hand, in the case of the C 1*s* annealed (600 °C) film, a new phase appeared at 287.45 eV, which is attributed to C–H/C–O–H bonding. The C 1*s* spectrum of the annealed film exhibits four peaks at 283.60, 285.54, 287.45, and 291.2 eV, which have been attributed to C–Si, C–C/C–H, C–O/C–O–H, and C=O bonds, respectively.^{16,26,27,30} Part of the oxygen is coming from di-

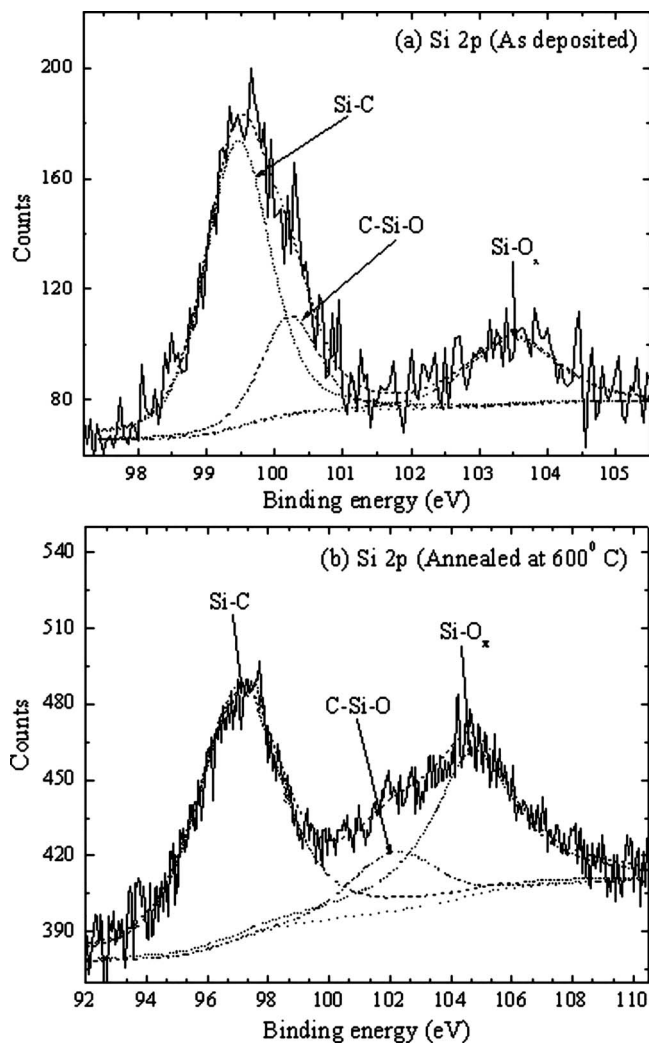


FIG. 6. Typical Si 2*p* spectra of SiCO:H film, (a) as deposited film and (b) annealed at 600 °C (CH₄/Ar=2:1, *f*=4 kHz, and *P*=300 mbar).

rectly connected to Si substrate (in the form of Si–O, SiO₂, or SiO₄) and the rest is coming from contamination of the air. The hydrocarbon layer covers major part of the Si substrate.

C. Fourier transform infrared spectroscopy

The absorption spectra of the as-deposited carbon film and RTA treatment of the same sample at 600 °C are shown in Fig. 8. A FTIR absorption measurement for the deposited sample was performed in the range between 500 and 4000 cm⁻¹. The absorption spectrum shows the different features. From Fig. 8, the vibrational spectrum of the as-deposited samples exhibits several peaks. Peaks at 610 and 742 cm⁻¹ are related to Si–O–Si(–CH₃) (or C–Si–CH₃) vibration,³¹ peaks at 890 cm⁻¹ attributed to Si–O–Si and Si–OH, peaks at 1108 cm⁻¹ assigned to Si–OC, peaks at 1372 and 1458 cm⁻¹ attributed to C–H_x vibrations,^{32–34} peaks at 1685 cm⁻¹ related to C=C vibration or C=O vibration,³⁵ peaks around 2931 cm⁻¹ assigned to the CH_x stretching vibrations^{36,37} and a broadband between 3200 and 3650 cm⁻¹ related to the OH vibration of silanol group and of adsorbed water. On the other hand the most of the corresponding peaks disappeared after annealing of the sample at

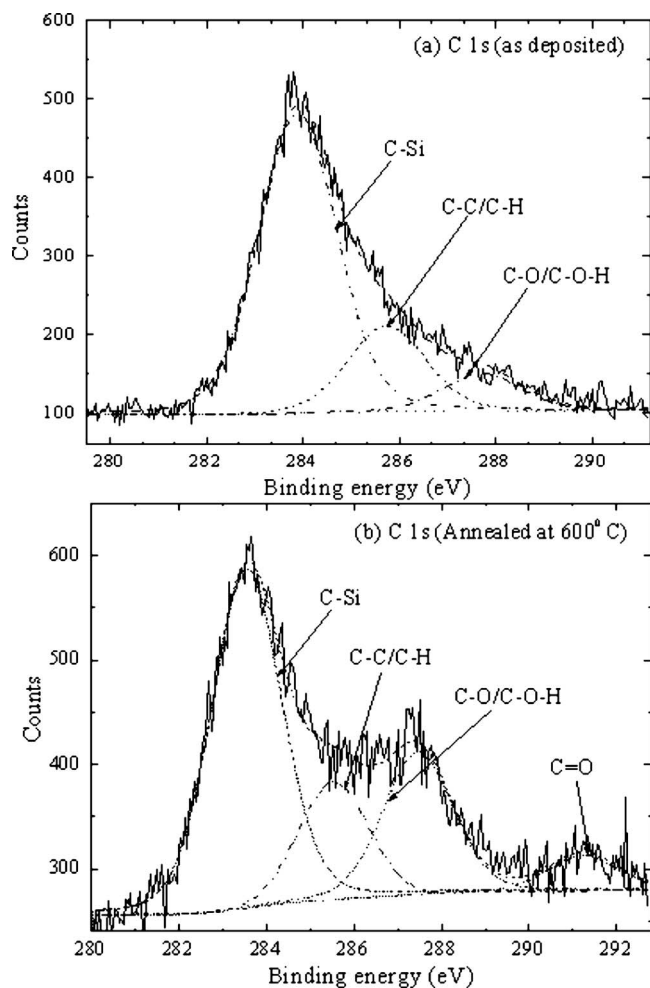


FIG. 7. Typical C 1s spectra of SiCO:H film, (a) as deposited film and (b) annealed at 600 °C ($\text{CH}_4/\text{Ar}=2:1$, $f=4$ kHz, and $P=300$ mbar).

600 °C. The peak at 682, 1378, and 2980 cm^{-1} were found in the case of annealed sample. The region between 600 and 800 cm^{-1} is a complex region,³⁸ where different vibration bands, Si–O–Si bending,³¹ Si–CH₃ rocking,³⁹ combination of Si–C stretching and SiC–CH₃ rocking modes, fall.⁴⁰ In as deposited film, the Si–O–Si band at around 1108 cm^{-1} is related to a cage structure with bond angle higher than 144°, whereas the Si–O–Si band at around 890 cm^{-1} is due to the network structure.³⁸ The peak at 1372 cm^{-1} is assigned to the formation of Si–CH₂–Si bridges.³⁴ Stapinski *et al.*^{1,10} mentioned that in the case of low concentration of carbon the appearing band at 682 cm^{-1} (in the case of 600 °C annealed sample) is due to the SiH_x wagging mode and the bands at 742 cm^{-1} , which are assigned to Si–CH₃ rocking/wagging mode or to Si–C stretching mode^{41,42} has the tendency to shift toward the higher wave number as the carbon concentration increases in the deposited film. The region between 2890 and 3000 cm^{-1} is due to CH_x stretching modes with *sp*² and *sp*³ bonding.¹⁰

From Eqs. (1)–(3), we can see that as the annealing temperature rises the organic to inorganic transformation of siloxane group networks approaches via radical reactions involving the cleavage of Si–C and C–H bonds with the consumption of Si–CH₃ groups (with the formation of gaseous species CH₄, H₂, and H₂O). Figure 8 shows that there is

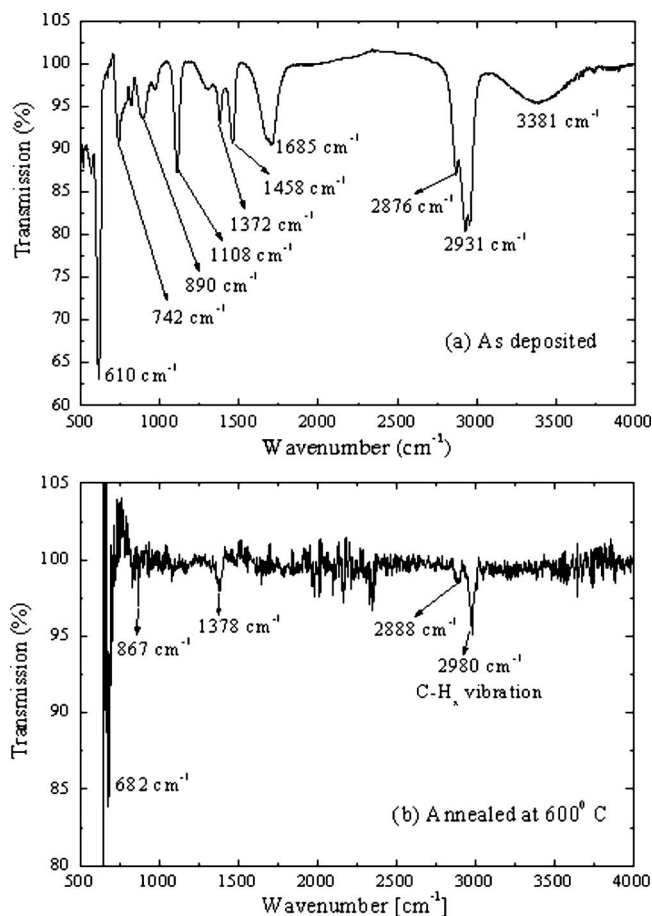
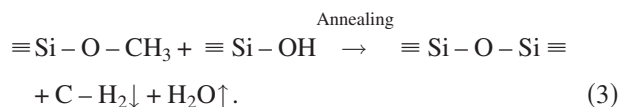
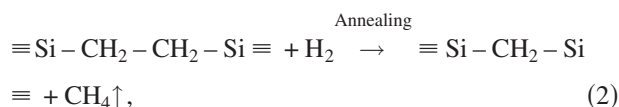
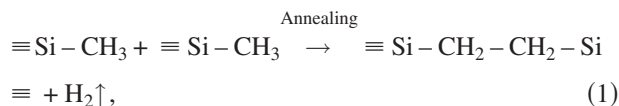


FIG. 8. Typical FTIR transmission spectra of deposited SiCO:H film in mixture of CH₄/Ar (2:1) where (a) is the as deposited film and (b) is the 600 °C annealed film.

a rapid change in the chemical bond structure of the film as the temperature rose up to 600 °C (obvious in SEM images). The observation of the FTIR spectra helps in understanding how carbon, hydrogen, and oxygen atoms are incorporated in the network with the formation of SiCO:H composite materials. The following reactions, which have extensively proposed in the formation in the literature, seem to apply to the present case,^{43,44}



From the above reactions mechanism, it is obvious that the deposited hydrocarbon film surface is partially evaporated and fragmented due to RTA in the neutral gas (Ar) medium. The migration of hydrogen atoms/molecules (as well as the evaporation of water molecules from the surface and substantial gas species, especially CH₄ gas) gave rise to the

bubble formation and growth. However, the hydrocarbon bubbles are formed due to the enhancement of the surface mobility and the surface tension of the Si wafer during plasma deposition. At elevated temperature the composition of the substrate becomes more relevant and the silicon content increases up to 62%.

IV. CONCLUSIONS

The presented results reveal the bubble-like structures formed (from SEM images, see Figs. 1–3) in the surface of deposited hydrogenated carbon film. The quantitative information obtained from the EDX spectra about the stoichiometry of the sample of O, C, and Si supports the XPS as well FTIR results. As the RTA temperature is increased from room temperature to 200 °C, the hydrocarbon bubbles started melting, however, the rate of melting is very small and when it was annealed at 600 °C, it started melting drastically and ultimately evaporating from the film surface. The hydrocarbon layer on silicon wafer, deposited by CH₄/Ar DBD, is not suitable to operate for higher temperature than 200 °C. For the hydrogenated carbon films, the influence of annealing process is not so straightforward and it needs further investigation.

ACKNOWLEDGMENTS

Part of this work was supported by the Deutsche Forschungsgemeinschaft (DFG) through Sonderforschungsbereich SFB/TR 24 “Fundamentals of Complex Plasmas” and by The International Max Planck Research School (IMPRS) “Bounded Plasmas.” We are thankful to Professor Tapas K. Chini and Mr. Souvik Banerjee of SINP, Kolkata, India for several discussions and SEM measurement, respectively.

- ¹I. Pereyra and M. N. P. Carreño, *J. Non-Cryst. Solids* **201**, 110 (1996); See, for example, *Amorphous and Crystalline Silicon Carbide*, Springer Proceedings in Physics, edited by G. L. Harris and C. Y.-W. Yang (Springer, New York, 1989) and *Amorphous and Crystalline Silicon Carbide*, Springer Proceedings in Physics, edited by G. L. Harris and C. Y.-W. Yang (Springer, New York, 1992).
- ²M. Mehregany, C. A. Zorman, S. Roy, A. J. Fleischman, C. H. Wu, and N. Rajan, *Int. Mater. Rev.* **45**, 85 (2000).
- ³J. B. Casady and R. W. Johnson, *Solid-State Electron.* **39**, 1409 (1996).
- ⁴M. Pozzi, M. Hassan, A. J. Harris, J. S. Burdess, L. Jiang, K. K. Lee, R. Cheung, G. J. Phelps, N. G. Wright, C. A. Zorman, and M. Mehregany, *J. Phys. D* **40**, 3335 (2007).
- ⁵L. Tong, M. Mehregany, and L. G. Matus, *Appl. Phys. Lett.* **60**, 2992 (1992).
- ⁶O. Kordina, L. O. Bjorketun, A. Henry, C. Hallin, R. C. Glass, L. Hulyman, J.-E. Sundgren, and E. Janzen, *J. Cryst. Growth* **154**, 303 (1995).
- ⁷R. F. Davis, J. W. Palmour, and J. A. Edmond, *Tech. Dig. - Int. Electron Devices Meet.* **90**, 785 (1990).
- ⁸H. Habuka, M. Watanabe, Y. Miura, M. Nishida, and T. Sekiguchi, *J. Cryst. Growth* **300**, 374 (2007).
- ⁹J. Kim and H. H. Lee, *Macromol. Mater. Eng.* **286**, 201 (2001).

- ¹⁰T. Stapinski and B. Swatowska, *J. Non-Cryst. Solids* **352**, 1406 (2006).
- ¹¹W. Xie, J. A. Cooper, Jr., and M. R. Melloch, *IEEE Electron Device Lett.* **15**, 455 (1994).
- ¹²*Properties of Silicon Carbide*, Emis Data Reviews Ser. No. 13, edited by G. L. Harris (INSPEC, IEEE, London, UK, 1995).
- ¹³W. K. Choi, Y. M. Chan, C. H. Ling, Y. Lee, R. Gopalakrishnan, and K. L. Tan, *J. Appl. Phys.* **77**, 827 (1995).
- ¹⁴A. Orpella, M. Vetter, R. Ferre, I. Martin, J. Puigdollers, C. Voz, and R. Alcubilla, *Sol. Energy Mater. Sol. Cells* **87**, 667 (2005).
- ¹⁵W. K. Choi, T. Y. Ong, L. S. Tan, F. C. Loh, and K. L. Tan, *J. Appl. Phys.* **83**, 4968 (1998).
- ¹⁶A. Majumdar, G. Das, N. Patel, P. Mishra, D. Ghose, and R. Hippler, *J. Electrochem. Soc.* **155**, D22 (2008).
- ¹⁷A. Majumdar, J. Schäfer, P. Mishra, D. Ghose, J. Meichsner, and R. Hippler, *Surf. Coat. Technol.* **201**, 6437 (2007).
- ¹⁸G. Borcia, C. A. Anderson, and N. M. D. Brown, *Surf. Coat. Technol.* **201**, 3074 (2006).
- ¹⁹A. Sonnenfeld, T. M. Tun, L. Zajikova, K. M. Kozlov, H. E. Wagner, J. F. Behnke, and R. Hippler, *Plasmas Polym.* **6**, 237 (2001).
- ²⁰O. Goossens, E. Dekempeneer, D. Vangeneugden, R. Van De Leest, and C. Leys, *Surf. Coat. Technol.* **142–144**, 474 (2001).
- ²¹S. Paulussen, R. Rego, O. Goossens, D. Vangeneugden, and K. Rose, *J. Phys. D* **38**, 568 (2005).
- ²²Y. H. Liu, J. Li, D. P. Liu, T. C. Ma, and G. Benstetter, *Surf. Coat. Technol.* **200**, 5819 (2006).
- ²³P. Heyse, R. Dams, S. Paulussen, K. Houthoofd, K. Janssen, P. A. Jacobs, and B. F. Sels, *Plasma Processes Polym.* **4**, 145 (2007).
- ²⁴A. Majumdar, J. F. Behnke, R. Hippler, K. Matyash, and R. Schneider, *J. Phys. Chem. A* **109**, 9371 (2005).
- ²⁵A. Majumdar and R. Hippler, *Rev. Sci. Instrum.* **78**, 075103 (2007).
- ²⁶J. Heo and H. J. Kim, *J. Electrochem. Soc.* **153**, F228 (2006).
- ²⁷M. R. Alexander, R. D. Short, F. R. Jones, W. Michaeli, and C. J. Blomfield, *Appl. Surf. Sci.* **137**, 179 (1999).
- ²⁸E. Riedo, F. Comin, J. Chevrier, F. Schmithusen, S. Decossas, and M. Sancrotti, *Surf. Coat. Technol.* **125**, 124 (2000).
- ²⁹A. Majumdar, G. Scholz, and R. Hippler, *Surf. Coat. Technol.* **203**, 2013 (2009).
- ³⁰X. Yan, T. Xu, G. Chen, S. Yang, H. Liu, and Q. Xue, *J. Phys. D* **37**, 907 (2004).
- ³¹G. Lucovsky, M. J. Manitini, J. K. Srivastava, and E. A. Irene, *J. Vac. Sci. Technol. B* **5**, 530 (1987).
- ³²G. Socrates, *Infrared Characteristic Group Frequencies* (Wiley, Chichester, 1994), Vol. 18, p. 186.
- ³³C. Pivin and P. Colombo, *J. Mater. Sci.* **32**, 6163 (1997).
- ³⁴S. Sugahara, T. Kadoya, K. Usami, T. Hattori, and M. Matsumura, *J. Electrochem. Soc.* **148**, F120 (2001).
- ³⁵C. K. Jung, D. C. Lim, H. G. Jee, M. G. Park, S. J. Ku, K. S. Yu, B. Hong, S. B. Lee, and J. H. Boo, *Surf. Coat. Technol.* **171**, 46 (2002).
- ³⁶N. Mutsukura, S.-I. Inoue, and Y. Machi, *J. Appl. Phys.* **72**, 43 (1992).
- ³⁷G. Das, G. Mariotto, and A. Quaranta, *J. Electrochem. Soc.* **153**, F46 (2006).
- ³⁸A. Grill and D. A. Neumayer, *J. Appl. Phys.* **94**, 6697 (2003).
- ³⁹Y.-H. Kim, M. S. Hwang, H. J. Kim, J. Y. Kim, and Y. Lee, *J. Appl. Phys.* **90**, 3367 (2001).
- ⁴⁰Y. W. Koh, K. P. Loh, L. Rong, A. T. S. Wee, L. Huang, and J. Sudijono, *J. Appl. Phys.* **93**, 1241 (2003).
- ⁴¹B. Mitu, G. Dinescu, M. Dinescu, A. Ferrari, and M. Balucani, *Thin Solid Films* **383**, 230 (2001).
- ⁴²T. Stapinski, G. Ambrosone, U. Coscia, F. Giorgis, and C. F. Pirri, *Physica B* **254**, 99 (1998).
- ⁴³K. Kamiya, A. Katayama, H. Suzuki, K. Nishida, T. Hashimoto, J. Mat-suoka, and H. Nasu, *J. Sol-Gel Sci. Technol.* **14**, 95 (1999).
- ⁴⁴D. Bahloul-Hourlier, J. Latournerie, and P. Dempsey, *J. Eur. Ceram. Soc.* **25**, 979 (2005).